

Learning-Based Sensor Scheduling for Delay-Aware and Stable Remote State Estimation

Nho-Duc Tran, Aamir Mahmood, Mikael Gidlund

Department of Computer and Electrical Engineering, Mid Sweden University, 851 70 Sundsvall, Sweden

Email: {nhoduc.tran, aamir.mahmood, mikael.gidlund}@miun.se

Abstract—Unpredictable sensor-to-estimator delays fundamentally distort what matters for wireless remote state estimation: not just freshness, but how delay interacts with sensor informativeness and energy efficiency. In this paper, we present a unified, delay-aware framework that models this coupling explicitly and quantifies a delay-dependent information gain, motivating an information-per-joule scheduling objective beyond age of information proxies (AoI). To this end, we first introduce an efficient posterior-fusion update that incorporates delayed measurements without state augmentation, providing a consistent approximation to optimal delayed Kalman updates, and then derive tractable stability conditions ensuring that bounded estimation error is achievable under stochastic, delayed scheduling. This conditions highlight the need for unstable modes to be observable across sensors. Building on this foundation, we cast scheduling as a Markov decision process and develop a proximal policy optimization (PPO) scheduler that learns directly from interaction, requires no prior delay model, and explicitly trades off estimation accuracy, freshness, sensor heterogeneity, and transmission energy through normalized rewards. In simulations with heterogeneous sensors, realistic link-energy models, and random delays, the proposed method learns stably and consistently achieves lower estimation error at comparable energy than random scheduling and strong RL baselines (DQN, A2C), while remaining robust to variations in measurement availability and process/measurement noise.

Index Terms—Sensor scheduling, Kalman filter, remote state estimation, delayed measurements.

I. INTRODUCTION

Wireless remote state estimation is widely used in a broad range of wireless sensor network applications, including industrial monitoring, autonomous systems, and smart infrastructure [1]. In these settings, numerous heterogeneous sensors monitor and report the system state over bandwidth- and energy-limited links. With such constraints, not every sensor can transmit in every slot; sensor scheduling (deciding who transmits when) is therefore central to achieving accurate, timely estimates under resource constraints. A practical complication is that sensor-to-estimator delays are random and sometimes large, which changes what *good scheduling* entails. Focusing on information freshness alone is insufficient [2]. Performance depends on how freshness, a time property describing how old a packet is when used, interacts with sensor informativeness, a measurement property that explains how much that packet can reduce uncertainty given the sensor’s characteristics and the estimator’s current uncertainty, and with energy cost.

Existing studies on sensor scheduling for remote state estimation typically optimize a single performance axis under simplified assumptions. For instance, accuracy-driven works

focus on estimation error alone, often under idealized delay models or single-sensor settings [3]. Energy-efficient scheduling has likewise been explored [4], but without accounting for how delays and staleness degrade the value of a received packet. Age-of-Information (AoI) formulations capture data freshness [5], yet they generally overlook random network delays that can render packets outdated upon arrival and do not account for sensor heterogeneity or energy cost.

While AoI equals the packet delay at the instant of reception, it is only a freshness proxy. The actual estimation gain depends jointly on the delay δ , the current error covariance \mathbf{P} , the sensor’s informativeness and energy usage E . In this respect, a plausible option is to schedule by maximizing an information-per-joule criterion $\Delta(\mathbf{P}, \delta)/E$ instead of minimizing AoI. However, to the best of our knowledge, despite significant progress in related domains, a comprehensive scheduling framework that jointly optimizes estimation accuracy, freshness, heterogeneity, energy use, and stochastic delays has not yet been established.

To address these gaps, in this work, we study a multi-sensor remote estimation problem in which heterogeneous sensors, differing in measurement model and noise level, observe a linear dynamical process over wireless links with stochastic sensor-to-estimator delays. We formulate a scheduling problem that explicitly accounts for estimation error, per-transmission energy, and the age-induced attenuation of measurement value via a delay-dependent information gain normalized by energy. Because scheduling in this setting is inherently combinatorial and dynamic, traditional optimization approaches become intractable.. We therefore adopt a reinforcement-learning (RL) formulation in which a policy selects, at each slot, which sensor (if any) should transmit to optimize a long-term objective that jointly balances estimation accuracy, energy consumption, and freshness. The main contributions of this paper are as follows:

- 1) We develop a delay-aware system model that captures the trade-offs among estimation accuracy, packet freshness, sensor heterogeneity, and energy consumption.
- 2) We derive stability conditions that yield the feasible bounded estimation error under delayed and stochastic scheduling, providing theoretical assurance of estimator reliability.
- 3) We design a reinforcement learning scheduler, based on PPO, where the state encodes estimation uncertainty and delay history, and the reward explicitly balances estimation improvement and transmission energy.

4) Through extensive simulations, we show that the proposed method outperforms random scheduling and other RL baselines such as DQN and A2C, with PPO achieving higher stability and performance under heavy delays.

The rest of the paper is organized as follows. Section II describes the system model and problem formulation. Section III details our approach to handling delayed measurements. The feasible stability condition and proposed scheduling algorithm are presented in Section IV, and Section V provides a thorough discussion of the simulation results. Finally, Section VI concludes the paper.

II. SYSTEM MODEL

As shown in Fig. 1, we consider a time-slotted wireless sensor network where M sensors monitor N states. Let $\mathcal{M} = \{1, \dots, M\}$ and $\mathcal{N} = \{1, \dots, N\}$ denote the sensor and state indices, respectively. The system state is $\mathbf{x}_k = [x_1(k), \dots, x_N(k)]^\top \in \mathbb{R}^N$. Each sensor $i \in \mathcal{M}$ observes m_i features of \mathbf{x}_k ($1 \leq m_i \leq N$), and generates a measurement $\mathbf{y}_k^i \in \mathbb{R}^{m_i}$ with probability p_i every time step. Since a single channel is shared, at most one sensor transmits per slot, determined by the scheduling signal from the remote estimator. When selected, sensor i sends its latest measurement, possibly acquired at $k - \delta$ ($\delta \geq 0$), and such delays can degrade estimation accuracy.

A. State Space Model

We adopt a discrete linear time-invariant (LTI) process-measurement model as the canonical abstraction for sampled-data systems. It provides the standard, analytically tractable baseline for rigorously characterizing delayed estimation and scheduling, including closed-form covariance evolution and stability conditions based on the observability of unstable modes. The posterior-fusion mechanism and the policy-learning approach extend to nonlinear processes via Extended Kalman Filter/Unscented Kalman Filter linearization, but we state formal guarantees for the LTI case, consistent with common practice in sampled-data control and estimation [6]. For an N -dimensional LTI system observed by M heterogeneous sensors, the state \mathbf{x}_k evolves as

$$\mathbf{x}_{k+1} = \mathbf{A} \mathbf{x}_k + \mathbf{w}_k, \quad \mathbf{w}_k \sim \mathcal{N}(0, \mathbf{Q}), \quad (1)$$

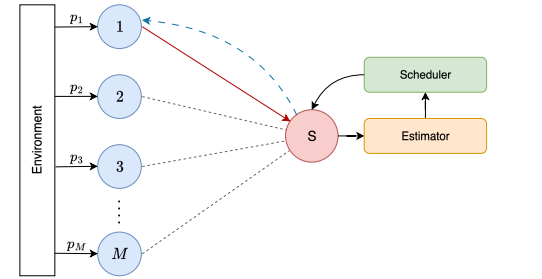
$$\mathbf{y}_k^i = \mathbf{C}_i \mathbf{x}_k + \mathbf{v}_k^i, \quad \mathbf{v}_k^i \sim \mathcal{N}(0, \mathbf{R}_i), \quad (2)$$

where $\mathbf{A} \in \mathbb{R}^{N \times N}$ is the state transition matrix, $\mathbf{C}_i \in \mathbb{R}^{m_i \times N}$ is the measurement matrix of sensor i , while the process noise \mathbf{w}_k and measurement noise \mathbf{v}_k^i are uncorrelated zero-mean Gaussian vectors with covariances $\mathbb{E}[\mathbf{w}_k \mathbf{w}_j^\top] = \delta_{kj} \mathbf{Q}$, $\mathbb{E}[\mathbf{v}_k^i (\mathbf{v}_j^i)^\top] = \delta_{kj} \mathbf{R}_i$, where $\delta_{kj} = 1$ if $k = j$ and 0 otherwise.

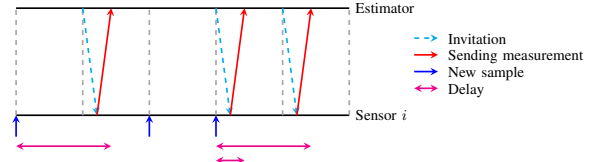
B. Scheduler

We define the binary variable γ_k^i to indicate whether the measurement \mathbf{y}_k^i from sensor i at time k is chosen:

$$\gamma_k^i = \begin{cases} 1, & \text{if } \mathbf{y}_k^i \text{ is selected,} \\ 0, & \text{if } \mathbf{y}_k^i \text{ is not selected.} \end{cases} \quad (3)$$



(a) Each sensor $i \in \mathcal{M}$ has a measurement matrix \mathbf{C}_i . With probability p_i , it generates a noisy measurement with covariance \mathbf{R}_i . The most recent measurement, possibly delayed by δ_k^i , is sent to the estimator at energy cost E^i if the invitation is received at time step k .



(b) Due to the randomness of new sample generation, the delay may vary depending on when sensor i is selected.

Fig. 1. Overview of network model and optimization problem. The question is which sensor (or none) is the best action at each time step.

At each time step k , the selection of sensors is captured by the vector $\boldsymbol{\gamma}_k = [\gamma_k^1 \ \gamma_k^2 \ \dots \ \gamma_k^M]$. Therefore, the general decision can be represented as $\theta = \{\boldsymbol{\gamma}_k\}_{k=1}^\infty$.

C. Estimation Model and Error Covariance

Denote the prior estimate of \mathbf{x}_k as $\hat{\mathbf{x}}_{k|k-1}$, and $\hat{\mathbf{x}}_{k|k}$ as the posterior estimate of \mathbf{x}_k after updating the measurement \mathbf{y}_k :

$$\hat{\mathbf{x}}_{k|k-1} \triangleq \mathbb{E}[\mathbf{x}_k | \mathbf{y}_{k-1}], \quad \hat{\mathbf{x}}_{k|k} \triangleq \mathbb{E}[\mathbf{x}_k | \mathbf{y}_k]. \quad (4)$$

In practical scenarios, acquiring the true system state for evaluating performance and making decisions is often infeasible. Therefore, we rely on the estimation error covariance matrix \mathbf{P} as a proxy for estimation accuracy. Specifically, \mathbf{P} with respect to $\hat{\mathbf{x}}_{k|k-1}$ and $\hat{\mathbf{x}}_{k|k}$ is given as

$$\mathbf{P}_{k|k-1} = \mathbb{E}[(\mathbf{x}_k - \hat{\mathbf{x}}_{k|k-1})(\mathbf{x}_k - \hat{\mathbf{x}}_{k|k-1})^\top], \quad (5)$$

$$\mathbf{P}_{k|k} = \mathbb{E}[(\mathbf{x}_k - \hat{\mathbf{x}}_{k|k})(\mathbf{x}_k - \hat{\mathbf{x}}_{k|k})^\top]. \quad (6)$$

D. Energy Consumption Model

In remote state estimation, heterogeneous and dispersed devices incur different costs for sending data to the remote estimator. We define the transmission-cost vector $\mathbf{E} = [E^1, E^2, \dots, E^M]$, where E^i follows the energy-limited sensor model. The total energy for transmitting N_b bits is [7]

$$E^i = (P_t + P_c) \frac{N_b}{B \log_2(1 + \rho_i)}, \quad \rho_i = \frac{\eta P_t G_i}{N_0 B}, \quad (7)$$

with P_t : transmit power, P_c : circuit/baseband power, B : bandwidth, G_i : channel gain, N_0 : noise spectral density, ρ_i : SNR of sensor i , and η : PA efficiency.

E. Problem Formulation

We aim to jointly optimize state estimation accuracy and sensor energy consumption in the presence of uncertain measurement delays by designing a scheduling policy θ that

minimizes the long-term average cost. Because these two metrics differ in scale and units, a direct combination would bias the optimization. To eliminate this imbalance, we apply min–max normalization to map both estimation error and energy cost into the range $[0, 1]$, leading to the formulation:

$$\min_{\theta} \lim_{T \rightarrow \infty} \frac{1}{T} \sum_{k=1}^T \left\{ \frac{\text{trace}(\mathbf{P}_k)}{\text{trace}(\mathbf{P}_0)} + \beta \gamma_k \frac{E_k}{\max \mathbf{E}}^\top \right\}. \quad (8)$$

In this study, the weighting parameter β is assumed to be fixed, while a general framework for multi-objective balancing is left for future work. Importantly, however, solving (8) requires evaluating how delayed measurements influence the evolution of \mathbf{P}_k . Accordingly, the next section develops a delay-aware posterior-fusion estimator and a delay-dependent information gain that will later drive scheduling decisions.

III. DELAY-AWARE STATE ESTIMATION METHODS

We begin with the standard Kalman prediction and update, then develop a delay-aware posterior-fusion estimator that incorporates delayed measurements without replay.

A. State Estimation

Every timestep, the estimator predicts the next state and error covariance of the system by

$$\hat{\mathbf{x}}_{k|k-1} = \mathbf{A} \hat{\mathbf{x}}_{k-1|k-1}, \quad (9)$$

$$\mathbf{P}_{k|k-1} = \mathbf{A} \mathbf{P}_{k-1|k-1} \mathbf{A}^\top + \mathbf{Q}. \quad (10)$$

When a timely measurement \mathbf{y}_k^i is available at time k , the filter calculates the Kalman gain, the posterior estimate state, and error covariance

$$\mathbf{K}_k = \mathbf{P}_{k|k-1} \mathbf{C}_i^\top (\mathbf{C}_i \mathbf{P}_{k|k-1} \mathbf{C}_i^\top + \mathbf{R}_i)^{-1}, \quad (11)$$

$$\hat{\mathbf{x}}_{k|k} = \hat{\mathbf{x}}_{k|k-1} + \mathbf{K}_k (\mathbf{y}_k^i - \mathbf{C}_i \hat{\mathbf{x}}_{k|k-1}), \quad (12)$$

$$\mathbf{P}_{k|k} = (\mathbf{I} - \mathbf{K}_k \mathbf{C}_i) \mathbf{P}_{k|k-1}. \quad (13)$$

B. Incorporating Delayed Measurement Updates

At time k , suppose a measurement from sensor i generated at $\tau = k - \delta_{i,k}$ arrives is: $\mathbf{y}_\tau^i = \mathbf{C}_i \mathbf{x}_\tau + \mathbf{v}_\tau^i$, $\mathbf{v}_\tau^i \sim \mathcal{N}(0, \mathbf{R}_i)$.

1) *Update at the generation time.* From the stored prior $(\hat{\mathbf{x}}_\tau, \mathbf{P}_\tau)$, we apply a standard Kalman update in (11)-(13) to find posterior $(\hat{\mathbf{x}}_{\tau|\tau}^{(i)}, \mathbf{P}_{\tau|\tau}^{(i)})$.

2) *Step-by-step propagation and fusion.* At each ensuing time instant j ($\tau < j < k$), the posterior $(\hat{\mathbf{x}}_{\tau|\tau}^{(i)}, \mathbf{P}_{\tau|\tau}^{(i)})$ is advanced forward by employing the prediction mechanisms (9)-(10). If another sensor's measurement has already been integrated at j , the advanced state $(\hat{\mathbf{x}}_j^p, \mathbf{P}_j^p)$ is amalgamated with the system's posterior $(\hat{\mathbf{x}}_{j|j}, \mathbf{P}_{j|j})$:

$$\mathbf{K}_j = \mathbf{P}_{j|j}^p (\mathbf{P}_{j|j}^p + \mathbf{P}_{j|j})^{-1}, \quad (14)$$

$$\hat{\mathbf{x}}_{j|j}^p = \hat{\mathbf{x}}_{j|j}^p + \mathbf{K}_j (\hat{\mathbf{x}}_{j|j} - \hat{\mathbf{x}}_{j|j}^p), \quad (15)$$

$$\mathbf{P}_{j|j}^p = (\mathbf{I} - \mathbf{K}_j) \mathbf{P}_{j|j}^p. \quad (16)$$

Instead of executing the filter from τ again by replaying delayed measurements, which, though optimal, remains impractical, our approach utilizes each posterior $(\hat{\mathbf{x}}_{j|j}, \mathbf{P}_{j|j})$

to represent all input data up to j in a Gaussian configuration. Considering this posterior as a virtual observation characterized by mean $\hat{\mathbf{x}}_{j|j}$ and covariance $\mathbf{P}_{j|j}$, we can integrate it with the delayed state, thus replaying data in a compressed form. Consequently, posterior fusion provides a practical and efficient approximation of complete updates, effectively utilizing all prior information without reprocessing.

3) *Final estimate at time k .* After iterating the propagate–fusion procedure until k , the corrected estimate $(\hat{\mathbf{x}}_{r|k}, \mathbf{P}_{r|k})$ is obtained. Its effect is quantified as $\Delta_i(\mathbf{P}_k, \delta_{i,k}) = \text{trace}(\mathbf{P}_{k|k-1}) - \text{trace}(\mathbf{P}_{r|k})$, which monotonically decreases with larger $\delta_{i,k}$.

IV. STABILITY ANALYSIS AND LEARNING-BASED SCHEDULING UNDER UNCERTAIN DELAYS

A. Stability Analysis

We say stabilization of the estimation error is *feasible* if there exists an admissible schedule θ such that

$$G = \sup_{\mathbf{P}_0 \geq 0} \limsup_{k \rightarrow \infty} \|\mathbb{E}(\mathbf{P}_k)\| < \infty.$$

Assuming, without loss of generality, that the state transition matrix \mathbf{A} is already in Jordan normal form, $\mathbf{A} = \mathbf{I}^{-1} \mathbf{A} \mathbf{I} = \text{diag}(\mathbf{A}_u, \mathbf{A}_s)$, then if $\rho(\mathbf{A}) < 1$, the system exhibits asymptotic stability even in the absence of measurement updates [8]. Conversely, let us consider $\rho(\mathbf{A}_u) \geq 1$, and denote $\bar{\mathbf{C}}_i := \mathbf{C}_i \mathbf{I} = [\mathbf{C}_i^u \ \mathbf{C}_i^s]$. The detectability of the system requires that its unstable modes be observable, which is equivalent to the existence of a schedule $\theta = \{\gamma_1, \gamma_1, \dots, \gamma_r\}$, $r = \dim(\mathbf{A}_u)$ such that matrix $[\mathbf{C}_{\gamma_1}^u, \mathbf{C}_{\gamma_2}^u \mathbf{A}_u, \dots, \mathbf{C}_{\gamma_r}^u \mathbf{A}_u^{r-1}]^\top$ has full rank.

Remark 1. Define $\mathcal{O} = [\mathbf{B}_0, \mathbf{B}_1, \dots, \mathbf{B}_{r-1}]^\top$ where $\mathbf{B}_i = [\mathbf{C}_1^u, \mathbf{C}_1^u, \dots, \mathbf{C}_M^u]^\top \mathbf{A}_u^i$. The unstable modes u of the system is observable only when

$$1) \text{rank}(\mathcal{O}) = r.$$

2) There exist vectors $\mathbf{b}_i \in \text{row}(\mathbf{B}_k)$ for each $i \in \{0, \dots, r-1\}$ such that $\{\mathbf{b}_0, \mathbf{b}_1, \dots, \mathbf{b}_{r-1}\}$ are linearly independent. Equivalently, for all i ,

$$\mathcal{R}_k = \text{row}(\mathbf{B}_i) \not\subseteq \sum_{j \neq i} \mathcal{R}_j, \quad \dim\left(\sum_{i=0}^{r-1} \mathcal{R}_i\right) = r.$$

B. Problem Analysis and Design Rationale

1) *Estimation Accuracy Dependencies:* The error covariance reduction when an update is received after a delay δ_k^i from sensor i is $\Delta_i(\mathbf{P}_k) = \mathbf{P}_{k|k-1} - \mathbf{P}_{k|k}$. Thus, $\Delta_i(\mathbf{P}_k, \delta)$ exhibits a non-increasing behavior in relation to δ and is bounded below by 0 in the absence of any updates. $\Delta_i(\mathbf{P}_k, \delta_1) \geq \Delta_i(\mathbf{P}_k, \delta_2) > 0$, $\delta_1 < \delta_2$. The $\Delta_i(\mathbf{P}_k)$ also depends on \mathbf{C}_i and \mathbf{R}_i . A sensor with large \mathbf{C}_i rank or small noise \mathbf{R}_i provides higher informativeness. Conversely, redundant or noisy sensors produce small Δ_i .

2) *Energy Consumption Dependencies:* The transmission energy of sensor i is fixed as E^i in (7). The efficiency of choosing sensor i is characterized by the benefit-to-cost ratio $\zeta_i(\mathbf{P}_k, \delta_k^i) = \Delta_i(\mathbf{P}_k, \delta_k^i) / \beta E^i$. For larger δ_k^i , the numerator

Δ_i shrinks, while different $\mathbf{C}_i, \mathbf{R}_i$ yield different Δ_i , and E^i also varies across sensors.

3) *Accuracy–Energy Trade-off*: Optimizing (8) therefore requires balancing: $\max_i \zeta_i(\mathbf{P}_k, \delta_k^i) = \max_i \Delta_i(\mathbf{P}_k, \delta_k^i)/\beta E^i$. This shows mathematically that freshness, heterogeneity, and random delays enter the problem implicitly, and that the optimal policy must jointly balance accuracy and energy through their combined effect.

C. MDP Formulation of the Scheduling Problem

We formulate the sensor scheduling problem as a Markov decision process (MDP) characterized as:

- *State Space*: At time step k , the state includes (i) the logarithm of the diagonal entries of the error covariance matrix, and (ii) the most recent ν sensor–delay pairs received by the estimator. Formally, $s_k = (\log(\text{diag}(\mathbf{P}_{k-1}) + \epsilon), (i, \delta)_{k-1:k-\nu})$, where $(i, \delta)_{k-1:k-\nu}$ denotes the sequence of the last ν sensor identifiers i and their associated delays δ . The state space is thus $\mathcal{S} = (\mathbb{R}^+)^N \times (\{0, 1, \dots, M\} \times \mathbb{R}^+)^{\nu}$.
- *Action Space*: At each time step k , the scheduler selects exactly one sensor or remains idle. We model this as a categorical action $\mathcal{A} = \{0, 1, \dots, M\}$, where $a_k = 0$ denotes idle and $a_k = i$ denotes scheduling sensor i .
- *Reward*: The reward at time step k is defined as $r_k = -\hat{u}_k - \beta \hat{e}_k$, where \hat{u}_k denotes the normalized uncertainty, \hat{e}_k the normalized energy consumption at time step k : $\hat{u}_k = \text{trace}(\mathbf{P}_k)/\text{trace}(\mathbf{P}_0)$, $\hat{e}_k = E_k/\max \mathbf{E}$. This formulation encourages the agent to minimize long-term estimation uncertainty while balancing the trade-off with energy consumption. The reward formulation implicitly enforces the stability feasibility condition: when observability of unstable modes is lost, the error covariance diverges, and the resulting large uncertainty term leads to strongly negative rewards.
- *Transition Dynamics*: The probability of state transition, as referenced in $\mathbb{P}(s_{k+1}|s_k, a_k)$, can be derived directly from the state updating rules delineated in (3), (9)–(16), in conjunction with the probabilistic assessments of each sensor as presented in p_i .

The state s_k captures (i) estimation uncertainty via the log of the covariance diagonal, ensuring scale invariance and avoiding dominance by large variances, and (ii) delay-awareness via the last ν sensor–delay pairs, summarizing recent staleness and scheduling history in a compact form.

D. Proximal Policy Optimization

Given the inherently continuous nature and high dimensionality of the state space, we utilize the proximal policy optimization (PPO) algorithm [9] to learn a stochastic policy, for its robustness and comparatively low hyperparameter sensitivity.

1) *The Actor*: The policy is represented by a neural network $\pi_\theta(a_t|s_t)$, which takes the current state s_t as input and outputs a probability distribution over possible actions that reflect equivalent accumulated reward in the future.

TABLE I
PARAMETERS FOR SIMULATION SETUP [7]

| Parameter | Symbol | Value |
|--------------------------------|------------|---------------------------|
| Number of bits to transmit | N_b | 280 |
| Bandwidth | B | 2 MHz |
| Transmit/receive-antenna gains | G_t, G_r | 1 |
| Wavelength | λ | 0.125 m |
| Distance | d_i | $\mathcal{U}(100, 300)$ m |
| Noise spectral density | N_0 | -174 dBm/Hz |
| Minimum SNR | ρ | 10 dB |
| Amplifier efficiency | η | 0.8 |
| Circuit/baseband power | P_c | 10 mW |
| Transmit power | P_t | 10 mW |
| Total time step | T | 100 |
| Weight coefficient | β | 0.1 |
| Sample probability | p_i | $\mathcal{U}(0.4, 0.6)$ |

2) *The Critic*: The value network $V_\phi(s_t)$ estimates the state value returns and updates by minimizing the mean squared error (MSE) between predicted $V_\phi(s_t)$ values and the empirical return \hat{R}_t .

3) *The update*: Both networks are trained jointly using the PPO objective, which combines three components: $L(\theta, \phi) = L_{\text{clip}}(\theta) + c_v L_{\text{value}}(\phi) - \beta_p H[\pi_\theta]$, where L_{clip} represents the clipped surrogate policy loss, L_{value} is the value function loss, and $H[\pi_\theta]$ (entropy) encourages exploration to avoid early convergence to deterministic policies. Coefficients c_v and β_p adjust the value and entropy weighting.

V. RESULTS AND DISCUSSION

A. Experimental Setup

We initialize the system described in Section II assuming a 5-dimensional state ($N = 5$) observed by $M = 20$ sensors. The state–space parameters are initialized as:

- $\mathbf{A} \in \mathbb{R}^{5 \times 5}$, $a_{ij} \sim \mathcal{U}[0, 1]$,
- $\mathbf{C}_i \in \mathbb{R}^{m \times 5}$, $c_{ij} \sim \mathcal{U}[-1, 1]$, $m \in [1, 5]$,
- $\mathbf{Q} = \mathbf{q}\mathbf{q}^\top + \epsilon \mathbf{I}$, $\mathbf{q} \in \mathbb{R}^{5 \times 5}$, $q_{ij} \sim \mathcal{U}[0, 1]$
- $\mathbf{R}_i = \mathbf{r}\mathbf{r}^\top + \epsilon \mathbf{I}$, $\mathbf{r} \in \mathbb{R}^{m \times m}$, $r_{ij} \sim \mathcal{U}[0, 1]$

The sensors are independently and uniformly deployed in an annulus with inner radius $d_{\min} = 100$ m and outer radius $d_{\max} = 300$ m. To focus on analyzing scheduling/aggregation effects, as in [10], the channel gain is abstracted by the Friis free-space model, $G_i = \frac{\lambda^2}{(4\pi d_i)^2} G_t G_r$, with λ the wavelength, d_i the sensor–receiver separation for sensor i , and G_t, G_r the transmit and receive antenna gains, respectively. Transmit powers are set to meet a target minimum SNR at the edge so that all scheduled packets are reliably received. Table I summarizes the wireless link-related simulation parameters.

B. Policy Learning Process

1) *Hyperparameter tuning*: We tuned the hyperparameters using the Optuna optimization framework [11]. A total of 50 trials, each comprising 10,000 steps, were executed to determine the optimal parameter set that yields the highest accumulated reward over 10 evaluation-phase episodes. Table II enumerates the tuned parameters, their respective ranges, and the achieved optimal values.

2) *Training phase*: At each iteration, N parallel environments generate rollouts of length T , forming a batch of $N \times T$ samples. The actor–critic networks process these trajectories, each implemented as a two-layer MLP with 128 and 64 hidden

TABLE II
PPO HYPERPARAMETER SEARCH SPACE AND SELECTED VALUES.

| Hyperparameter | Search Range | Optimal Value |
|------------------------|-------------------------------|----------------------|
| Learning rate | $[10^{-8}, 10^{-3}]$ | 1.9×10^{-4} |
| Discount factor | $[0.90, 0.99]$ | 0.94 |
| Clip coefficient | $[0.01, 0.5]$ | 0.18 |
| Entropy coefficient | $[10^{-4}, 2 \times 10^{-2}]$ | 0.01 |
| Number of environments | $\{4, 8, 16, 32\}$ | 16 |
| Number of steps | $[64, 2048]$, step = 64 | 192 |
| Number of minibatches | $[4, 64]$, step = 4 | 28 |
| Update epochs | $[4, 128]$, step = 8 | 108 |
| GAE λ | $[0.80, 0.99]$ | 0.98 |

units, respectively, to produce action probabilities and value estimates. Adam is used as the optimizer, and training proceeds for 10^6 environment steps. As shown in Fig. 2, the reward curve improves steadily with bounded fluctuations, reflecting stable learning. Fig. 3 shows that the policy loss oscillates around zero while the value loss converges after an initial transient, confirming that PPO achieves reliable and stable convergence in our setting.

C. Scheduling Policy Performance

We evaluate the performance of the proposed PPO-based scheduling policy against three baselines: random, Deep Q-Network (DQN)-based, and Advantage Actor–Critic (A2C)-based. To account for the stochastic nature of the environment and random packet delays, each method is simulated over 10^3 independent runs with the same random seeds.

1) *Baseline Comparison*: As shown in *Standard* column of Table III, PPO achieves the lowest mean cost and smallest variance of the objective value, indicating both efficiency and stability. PPO naturally learns to maintain bounded estimation error, operating within the stability-feasible region derived in Section IV-A. In contrast, random scheduling performs worst, as expected for its delay-energy-agnostic scheduling approach. Interestingly, while DQN approaches PPO in mean performance, its variance remains much higher, confirming its instability under stochastic delays. A2C provides more consistent results than DQN but falls short of PPO in both accuracy and robustness. See Sec. V-C3 and the remaining Table III columns for parameter-variation results.

Figure 4 and Fig. 5 present the progression of the trace of the error covariance $\text{trace}(\mathbf{P}_k)$ and the energy consumption E_k , respectively, over 100 time steps. Random scheduling is inadequate in leveraging informative sensors optimally, leading to consistently elevated uncertainty despite minimal energy consumption over time. Conversely, PPO consistently reduces the estimation error more effectively than all other baselines while maintaining competitive energy usage. Its energy consumption surpasses that of random scheduling, which is logical since it signifies the necessity of utilizing more energy than the average to achieve the desired accuracy. This observation aligns with the theoretical trade-off established in Sec. IV-B, where PPO efficiently balances the information gain $\Delta_i(\mathbf{P}, \delta)$ against the costs associated with sensor energy. Meanwhile, DQN exhibits pronounced fluctuations, whereas A2C produces comparatively smoother curves; however, it does not attain the low-error regime achieved by PPO.

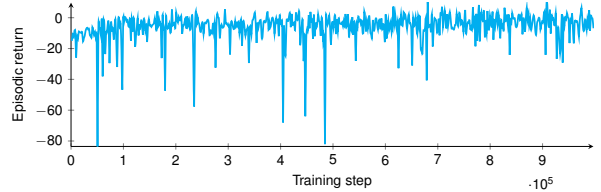


Fig. 2. PPO Reward learning curve

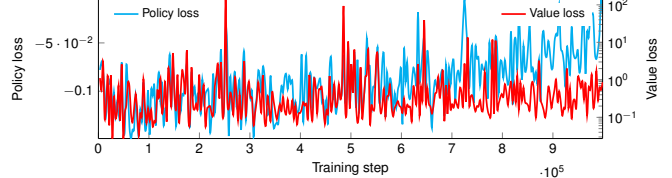


Fig. 3. PPO training loss

2) *Insights into Scheduling Dynamics*: To better understand why PPO outperforms alternatives, we inspect a single representative run of the agent in Fig. 6a, revealing how PPO balances estimation uncertainty and sensor energy usage.

- When $\text{trace}(\mathbf{P})$ is large, PPO prioritizes highly informative sensors with relatively low transmission energy (e.g., sensor 5, 17), quickly reducing estimation error at minimal cost.
- As uncertainty decreases, PPO begins to schedule a broader set of sensors, suggesting it improves estimation across all five state dimensions, not only relying on the most informative sensors. At this stage, delay becomes more critical, the agent often trades off between informativeness, energy, and packet staleness, as represented by $\zeta_i(\mathbf{P}, \delta) = \Delta_i(\mathbf{P}, \delta)/\beta E^i$.
- Once estimation stabilizes, PPO reduces the number of active sensors and primarily schedules a small set of low-cost, moderately informative sensors. This shows that PPO learns to maintain accuracy with minimal energy expenditure.

Fig. 6b compares theoretical and empirical average delays. In most cases, PPO lowers the delay compared to theory. However, for a few sensors (e.g., sensor 8, 11, 17 and 19), PPO occasionally chooses an action that results in a higher delay. This highlights that PPO is not entirely conservative: it sometimes takes “risky actions” if the expected information gain outweighs the delay penalty. This observation confirms the theoretical expectation of an exploration, exploitation trade-off, while also showing that PPO remains primarily risk-averse overall.

3) *Robustness to Parameter Variations*: Finally, we examine the robustness of each scheduling policy to changes in system parameters. In Table III, we vary (i) probability of new measurements, (ii) process noise covariance, and (iii) measurement noise covariance.

a) *Measurement generation probability*: When p_i decreases (measurements become less frequent and delays increase), all methods perform worse, with higher mean and variance of the objective. PPO and A2C adapt relatively well, whereas DQN suffers significantly for its value-based nature being less suited to stochastic environments. Random scheduling also degrades, but not as sharply as DQN. When p_i

TABLE III

PERFORMANCE COMPARISON OF SCHEDULING METHODS UNDER PARAMETER VARIATIONS. EACH ELEMENT REPRESENTS THE MEAN AND STANDARD DEVIATION OVER 1000 SIMULATION RUNS.

| Method | Standard | p_i variation | | q_{ij} variation | | r_{ij} variation | |
|--------|--------------------------------|-----------------------------|--------------------------------|--------------------------------|----------------------|--------------------------------|--------------------------------|
| | | $\mathcal{U}(0.1, 0.3)$ | $\mathcal{U}(0.7, 0.9)$ | $\mathcal{U}(0, 0.1)$ | $\mathcal{U}(1, 10)$ | $\mathcal{U}(0, 0.1)$ | $\mathcal{U}(1, 10)$ |
| Random | $0.17 \pm 1.73 \times 10^{-1}$ | $4.00 \pm 2.04 \times 10^1$ | $0.11 \pm 7.75 \times 10^{-3}$ | $0.10 \pm 7.75 \times 10^{-3}$ | 6.03 ± 5.13 | $0.15 \pm 2.24 \times 10^{-1}$ | $0.50 \pm 3.74 \times 10^{-1}$ |
| PPO | $0.13 \pm 2.45 \times 10^{-2}$ | $2.10 \pm 7.36 \times 10^0$ | $0.07 \pm 4.47 \times 10^{-3}$ | $0.08 \pm 1.00 \times 10^{-2}$ | 3.68 ± 1.22 | $0.12 \pm 1.41 \times 10^{-2}$ | $0.25 \pm 8.37 \times 10^{-2}$ |
| DQN | $0.15 \pm 7.75 \times 10^{-2}$ | $13.1 \pm 1.64 \times 10^2$ | $0.10 \pm 1.73 \times 10^{-2}$ | $0.12 \pm 2.83 \times 10^{-2}$ | 5.92 ± 3.26 | $0.15 \pm 7.07 \times 10^{-2}$ | $0.25 \pm 2.24 \times 10^{-1}$ |
| A2C | $0.14 \pm 6.32 \times 10^{-2}$ | $2.22 \pm 9.82 \times 10^0$ | $0.11 \pm 2.17 \times 10^{-2}$ | $0.07 \pm 1.79 \times 10^{-2}$ | 3.62 ± 2.93 | $0.14 \pm 3.87 \times 10^{-2}$ | $0.43 \pm 2.74 \times 10^{-1}$ |

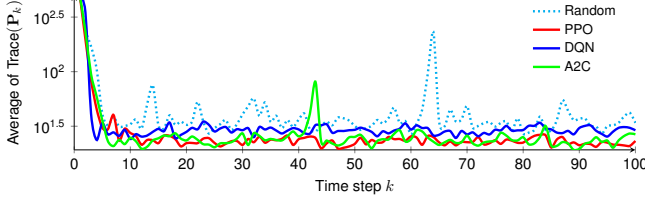


Fig. 4. Comparison of the average estimation error at each step over 100 steps (averaged across 1000 trials) for different scheduling policies.

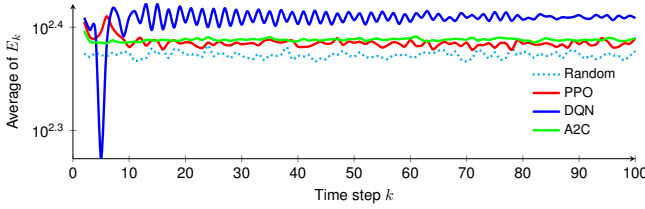


Fig. 5. Comparison of the energy consumption at each step over 100 steps (averaged across 1000 trials) for different scheduling policies.

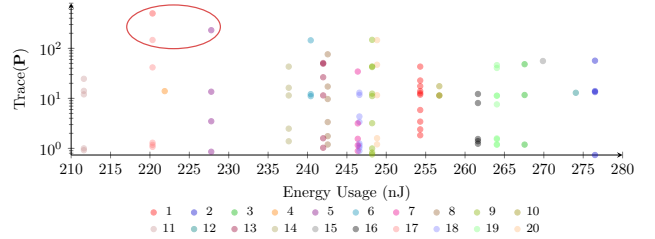
increases toward 0.7–0.9, results improve across all methods, approaching the *Standard* case.

b) *Process noise*: Reducing \mathbf{Q} makes the system model more accurate, which stabilizes estimation. As expected, all methods show improved performance with lower variance. Increasing \mathbf{Q} makes the system rely more heavily on sensor updates. Here, PPO and A2C still outperform, while DQN follows the same relative order as in the *Standard* case but with amplified variance. This is consistent with theory, as actor-critic methods (e.g., PPO, A2C) are better at adapting to noise-dominated regimes.

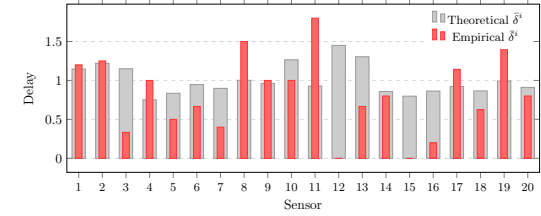
c) *Measurement noise*: When \mathbf{R}_i decreases, measurements are more accurate, making scheduling easier for all methods; conversely, larger \mathbf{R}_i , reduces informativeness and degrades performance. Unlike p_i and \mathbf{Q} , \mathbf{R}_i variations affect measurement quality directly rather than delay stochasticity. Accordingly, PPO and A2C retain superiority but with smaller relative gains, while DQN/random degrade as expected.

VI. SUMMARY

This work introduced two main contributions: a delay-aware estimator that maintains stability under delayed updates, and a PPO-based scheduler that optimally balances accuracy, energy, heterogeneity, and freshness. Together, they form a unified framework for reliable remote state estimation in delay-prone wireless networks. Our analysis establishes conditions for possible stability, providing theoretical insight, while simulations demonstrate strong empirical performance and robustness compared to other baselines. Future work will extend this framework toward adaptive multi-objective optimization for diverse IoT and industrial applications.



(a) Estimation uncertainty and energy usage trade off. For example, sensors 5 and 17 (circled in red) are selected during high-uncertainty phase, where PPO prioritizes highly informative and energy-efficient sensors to reduce estimation error rapidly.



(b) Comparison of average delay $\bar{\delta}^i$ between theory and simulation

Fig. 6. Demonstration in a single run of PPO-based policy in terms of optimizing and trade off between trace of error covariance, energy consumption, sensor heterogeneity, and information freshness.

REFERENCES

- [1] M. Trigka and E. Dritsas, "Wireless sensor networks: From fundamentals and applications to innovations and future trends," *IEEE Access*, vol. 13, pp. 96 365–96 399, 2025.
- [2] J. Luo and N. Pappas, "On the role of age and semantics of information in remote estimation of Markov sources," 2025, <https://arxiv.org/abs/2507.18514>.
- [3] S. Chandrasekaran *et al.*, "Distributed state estimation for linear time-varying systems with sensor network delays," in *European Control Conference (ECC)*, 2023, pp. 1–6.
- [4] X. Cao *et al.*, "Optimal sleep scheduling for energy-efficient AoI optimization in industrial internet of things," *IEEE Internet Things J.*, vol. 10, no. 11, pp. 9662–9674, 2023.
- [5] T. Chang *et al.*, "A lightweight sensor scheduler based on AoI function for remote state estimation over lossy wireless channels," *IEEE Trans. Automat. Contr.*, vol. 69, no. 3, pp. 1697–1704, 2024.
- [6] B. Zhou *et al.*, "Data-driven analysis methods for controllability and observability of a class of discrete LTI systems with delays," in *IEEE DDCLS*, 2018, pp. 380–384.
- [7] W. Yang *et al.*, "Minimum energy to send k bits over multiple-antenna fading channels," *IEEE Trans. Inf. Theory*, vol. 62, no. 12, pp. 6831–6853, 2016.
- [8] D. Simon, *Optimal State Estimation: Kalman, H Infinity, and Nonlinear Approaches*. USA: Wiley-Interscience, 2006.
- [9] J. Schulman *et al.*, "Proximal policy optimization algorithms," 2017. [Online]. Available: <https://arxiv.org/abs/1707.06347>
- [10] B. Sun *et al.*, "AoI-based optimal transmission scheduling for multi-process remote estimation," *IEEE Trans. Automat. Contr.*, 2025.
- [11] T. Akiba *et al.*, "Optuna: A next-generation hyperparameter optimization framework," in *Proceedings of the 25th ACM SIGKDD International Conference on Knowledge Discovery and Data Mining*, 2019.